Photopatterning of Stable, Low-Density, Self-Assembled Monolayers on Gold

ARTICLE *in* LANGMUIR · FEBRUARY 2015

Impact Factor: 4.46 · DOI: 10.1021/acs.langmuir.5b00001 · Source: PubMed

2 AUTHORS:

Leila Safazadeh
University of Kentucky
3 PUBLICATIONS **5** CITATIONS
SEE PROFILE

Brad J. Berron
University of Kentucky
23 PUBLICATIONS **224** CITATIONS
SEE PROFILE

Langmuir

Article

pubs.acs.org/Langmuir

Photopatterning of Stable, Low-Density, Self-Assembled Monolayers on Gold

Leila Safazadeh and Brad J. Berron*

Chemical and Materials Engineering, University of Kentucky, Lexington, Kentucky 40506-0046, United States

Supporting Information

ABSTRACT: Photoinitiated thiol−yne chemistry is utilized as a click reaction for grafting of acid-terminated alkynes to thiol-terminated monolayers on a gold substrate to create stable, low-density monolayers. The resulting monolayers are compared with a well-packed 11-mercaptoundecanoic acid monolayer and the analogous low-density monolayers prepared through a solution phase synthetic approach. The overall structuring of the monolayer prepared by solid-phase grafting is characterized by contact angle goniometry and Fourier transform infrared spectroscopy. The results show that the product monolayer has an intermediate surface energy and a more disordered chemical structuring compared to a traditional well-packed self-assembled monolayer, showing a low-packing density of the chains at the monolayer surface. The monolayer's structure and electrochemical stability were studied by reductive desorption of the thiolates. The prepared low-density monolayers have a higher electrochemical stability than traditional well-packed monolayers, which results from the crystalline structure at the gold interface. This technique allows for simple, fast preparation of low-density monolayers of higher stability than well-packed monolayers. The use of a photomask to restrict light access to the substrate yielded these low-density monolayers in patterned regions defined by light exposure. This general thiol−yne approach is adaptable to a variety of analogous low-density monolayers with diverse chemical functionalities.

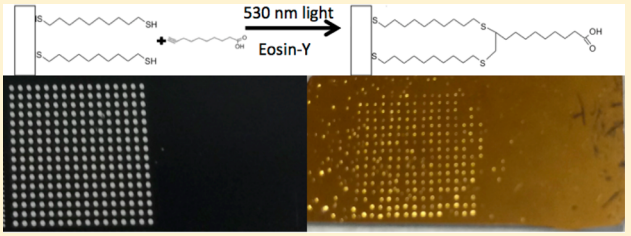

INTRODUCTION

Self-assembled monolayers (SAMs) are organic assemblies formed by the adsorption of molecular species from solution onto the surface of solids.[1,2] These adsorbates organize spontaneously into structurally well-defined and stable surfaces[3,4] that have been widely used for studies in surface modification and surface interactions.[2,5] The adsorbate molecules consist of headgroups with a specific affinity for a substrate and tail groups of different functionalities at the exposed interface.[6] Self-assembled monolayers of alkanethiolates on gold are among the most popular classes of SAMs.[4,7,8] The high affinity of alkanethiols for gold surfaces,[9] the inert properties of gold, and the versatility of thiol chemistry make it possible to construct well-defined surfaces of numerous chemical functionalities.[7,10]

While the crystalline structuring of traditional SAMs produces highly stable surface modifications, there are numerous applications where SAMs with more conformational freedom of functional groups are desired.[11,12] In particular, the interaction of proteins and other macromolecules with a surface of low chain density is distinct from interactions with traditional, densely-packed SAMs. In the seminal work of Choi et al.,[13] low chain density SAMs bound to human serum albumin more tenaciously than a densely-packed SAM. While similar phenomena are expected in other protein/SAM interactions, there are few stable, low-density monolayer systems available for these studies.[14−16]

We recently developed a unique synthetic approach toward low-density monolayers (LD-SAMs) on gold using the solution-phase synthesis of a Y-shaped adsorbate by a two to one thiol to yne addition reaction (Figure 1b).[7] When millimolar solutions of these adsorbates are contacted with gold substrates, a self-assembled monolayer forms with a layered structure. The layer interfacing the environment has a chain density roughly half that of a well-packed monolayer.[7] While many other techniques for low-density monolayers have been described,[17] the 2:1 covalent bond and densely packed underlying monolayer provide significant improvements in stability over the alternative low-density monolayer systems (Figure 1c,d).[18] The resulting LD-SAMs are even more electrochemically stable than a well-packed 11-mercaptohexadecanoic SAM, which is a first for in LD-SAMs.[7,19] Further, this system is based on thiol−yne click chemistry,[20−22] enabling the synthesis of low-density adsorbates of many functional groups. All other low-density monolayer synthesis approaches are tailored to one or two possible functional groups.[14−17,23]

Despite advantages in stability and adaptability, our previous approach fails to achieve the synthetic simplicity of alternative LD-SAM methods. In particular, the electrostatic methods developed by the Frechette group are staggeringly simple.[17] The carboxylate groups of mercaptohexadecanoic acid are

Received: January 1, 2015
Revised: February 16, 2015

DOI: 10.1021/acs.langmuir.5b00001
Langmuir XXXX, XXX, XXX−XXX

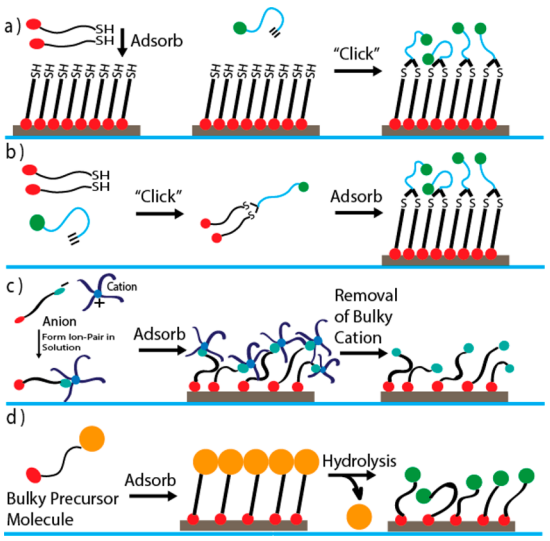

Figure 1. Schematic description of LD-SAM preparation processes. (a) Solid-phase synthesis of LD-SAMs composed of thiol−yne adsorbates. (b) Solution-phase synthesis of LD-SAMs composed of thiol−yne adsorbates. (c) Supermolecular ion-pair synthesis of LD-SAMs. (d) LD-SAM synthesis through adsorption of molecules and subsequent cleavage of bulky groups.

paired with bulky cations prior to substrate immersion (Figure 1c). In their approach, chain spacing is dictated by electrostatically bound cations. Upon cleavage of the bulky cations, the remaining mercaptohexadecanoic acid adsorbates are at a lower lateral density than conventional monolayers.[19] The Frechette group's two-step approach is advantageous in that it lacks solution phase synthesis and purification, while our previous thiol−yne approach offers greater stability of the adsorbate and a larger library of potential functional groups, including carboxylate, methyl, alcohol, and amine functionalities.

Here, we present a simplified synthetic strategy for stable, adaptable, low-density monolayers based on Y-shaped, thiol−yne adsorbates (Figure 1a). We utilize a solid phase synthesis of the monolayer through the deposition of a well-packed alkane dithiol monolayer followed by the addition of up to one alkyne tail group for every two surface-immobilized thiol groups. The resulting monolayers simultaneously provide both high stability and low chain packing density through a layered, doubly bound structure. The high density of head phase[9] and chelated structure[24] increase the energetic barrier to chain desorption from the gold surface and also prevents the loss of tail group spacing. Loss of tail group spacing is a significant challenge in some previous LD-SAM approaches, where the monolayer restructures into domains of densely packed chains.[18] This restructuring is primarily driven by the lack of van der Waals interactions between laterally spaced chains, where the backfilling other LD-SAM structures has increased the stability of these LD-SAM structures.[19] In contrast, the present work uses a densely packed lower layer to sterically prevent the restructuring of the environment-interfacing layer of reduced lateral packing density.

The solid phase grafting approach (Figure 1a) parallels the solution phase approach of our prior work (Figure 1b),[7] but the solid-phase approach simplifies adsorbate purification. For a solution phase synthesis, all sulfur-containing side products must be removed prior to SAM formation. While radical mediated thiol−yne addition is highly specific in the presence of many functional groups, the ditihiol reactant alone is prone to formation of oligomer and disulfide products.[21,22] A solid phase approach eliminates the purification challenges associated with the solution phase synthesis.[25] The highly crystalline, thiol-presenting surface of the precursor dithiol monolayer prevents the formation of undesired side products, while unreacted alkyne species materials are simply rinsed away after reaction.

Solid phase synthetic approaches are not without limitation, as 100% grafting is difficult to attain.[11] Further, the solvents used in the grafting process may destabilize the underlying dithiol monolayer.[4] Our experimental approach investigates each of these limitations. We quantify the grafting efficiency through surface energy analysis and ellipsometric thickness, while the destabilization of the underlying monolayer is investigated through impedance analysis and the electrochemical stability of the solid phase LD-SAM.

In addition to a simplified reaction scheme, the light-mediated aspect of grafting gives several unique advantages over our prior solution phase approach. First, the reaction time is easily controlled through irradiation time, allowing fine-tuning of reaction conditions. As radical life times in similar photoinitiated systems are on the order of microseconds,[26−28] the reaction time can be controlled to well below 1 s. Second, the surface modification only proceeds in the presence of light, allowing patterning of low-density monolayers on gold with the use of standard photomasks. Previous "adsorb and cleave" LD-SAM methods (Figure 1c,d) are incompatible with photopatterning. The simplest approach to patterning these conventional LD-SAM chemistries is to pattern the underlying metal, requiring additional materials processing. Thus, this work also represents the first low-density monolayer chemistry capable of being deposited in arbitrary patterns on a uniform surface of gold.

EXPERIMENTAL SECTION

Materials. 1,10-Decanedithiol (98%) was obtained from TCI America. *n*-Hexane (>95%), 10-undecynoic acid (95%), ethanol (>99.5%), potassium hexacyanoferrate(III) (>99%), potassium hexacyanoferrate(II) (>99.99%), sodium sulfate (>99%), 11-mercaptoundecanoic acid (MUA; 95%), and eosin Y (>99%) were purchased from Sigma-Aldrich (St. Louis, MO) and were used as received. Deionized, ultrafiltered water was purchased from Fisher Scientific. Silicon wafers (P/boron ⟨100⟩), 150 ± 0.2 mm diameter, with thickness of 600−650 μm and resistivity of <0.4, were obtained from WRS Materials. The photomask used for surface patterning was a chrome-coated glass mask purchased from Louisville Photomask. Solution-phase product LD-SAM was prepared as described previously.[7]

Gold Substrate Preparation. Gold-coated silicon wafers with chromium adhesion layers were prepared using a Hummer 8.1 dc sputter system. Silicon wafers were plasma cleaned and then placed into the sputter system chamber, where chromium (10 nm) and gold (50 nm) were sequentially deposited onto silicon wafers. The gold substrates were typically cut to 1 × 3 cm, rinsed with ethanol, and dried under a stream of N_2 prior to use.

Monolayer Preparation. Solid-phase low-density monolayers were prepared by immersing the clean gold substrates in a 1 mM solution of 1,10-decanedithiol in hexane for 24 h at room temperature to form SAMs. The samples were then rinsed in 1 mM aqueous dithiothreitol for 20 min to eliminate the presence of disulfides on the monolayer surface. Samples were rinsed with ethanol, followed by a brief rinse with deionized water and then ethanol, and then dried with a stream of N_2 prior to the grafting reaction. The substrates were then transferred to a round Pyrex petri dish, containing 3 mL of an ethanolic solution of 10-undecynoic acid (50 mM) and eosin Y (2.5

DOI: 10.1021/acs.langmuir.5b00001
Langmuir XXXX, XXX, XXX−XXX

mM) and 20% DI water, where they were irradiated with 530 nm light (THORLabs LED model M530L3, 10 mW/cm^2) for 7 min at room temperature. The illumination time was selected as long enough to promote the grafting reaction (as determined by surface energy and ellipsometry) and not sufficiently long to promote a breakdown of the underlying dithiol monolayer (as determined by lowering of film resistance by EIS). The irradiated substrates were sequentially rinsed with ethanol, deionized water, and ethanol and dried with a stream of N_2 gas prior to measurement. Solution-phase low-density monolayers were prepared according to our previously described method.[7]

Fourier Transform Infrared Spectroscopy (FTIR). The FTIR spectrometer is an Agilent 680 with an MCT detector, which is equipped with a universal sampling accessory for grazing angle analysis of thin organic coatings on metal surfaces. For SAM measurements, spectra were collected using 100 scans at an incident angle of 80° from the surface normal using plasma cleaned gold substrate as a background. Data are from at least three measurements on at least four samples, and the values are reported as the mean ± standard deviation.

Electrochemical Impedance Spectroscopy (EIS). Electrochemical measurements were performed using a standard three-electrode electrochemical flat cell (Princeton Applied Research, model K0235) using a Gamry potentiostat (Reference 600). The substrates were mounted to the flat cell with a fixed working electrode area of 1 cm^2. An Ag/AgCl/saturated KCl(aq) was used as a reference electrode and a bare gold-coated silicon substrate as a counter electrode. EIS data were acquired in an electrolyte solution of 1 mM $K_3[Fe(CN)_6]$, 1 mM $K_4[Fe(CN)_6]$, and 0.1 M Na_2SO_4 by scanning between 10^{-1} and 10^4 Hz, and all impedance spectra were taken at an open circuit potential and an ac modulation of 10 mV. A Randles equivalent circuit was fit to data to determine resistance and capacitance values. All experiments were conducted at room temperature. Data are from at least nine samples, and the values are reported as the mean ± standard deviation.

Reductive Desorption. Electrochemical measurements were taken using the same apparatus as for EIS. Cyclic voltammograms were acquired in 0.5 M KOH while the potential was cycled starting from 0.345 to −1.545 V (vs Ag/AgCl), at scan rate of 100 mV/s, with at least two cycles. All experiments were conducted at room temperature after deaerating the electrolyte with ultrapure nitrogen gas for 1 h. After each measurement the position and area of desorption peaks of the first sweep were calculated. The desorption peak area represents the total charge required to reduce all of the thiol−Au bonds in 1 cm^2 of the SAM and was calculated from a Gaussian fit to experimental data. The total charge required to remove the SAM is then used to quantitatively determine the density of thiol−gold bonds at the gold−monolayer interface $\Gamma_{Au\text{-}SR}$ (eq 1).

$$\Gamma_{Au-SR} = \frac{Q_{Au-SR}}{nFA} \quad (1)$$

where $Q_{Au\text{-}SR}$ is the total charge in the desorption peak, n is the number of electrons involved in the electron-transfer process (n = 1 for this reaction), F is the Faraday constant, and A is the electrode surface area exposed to the alkaline solution. Data are from at least three measurements on at least nine samples, and the values are reported as the mean ± standard deviation.

Spectroscopic Ellipsometry. Monolayer thicknesses were determined ellipsometrically (M-2000, J.A. Woollam Co. Inc.). Polarization data were taken from 245 to 725 nm at incident angles every 2° between 65° and 75° from the surface normal. Thicknesses and optical constants were fit to experimental data using a standard Cauchy model. Optical constants used for the measurements were obtained for the underlying gold substrate used in preparation of monolayers. Data are from at least three measurements on at least nine samples, and the values are reported as the mean ± standard deviation.

Static Contact Angle Goniometry. Static water contact angles were measured with a Rame-Hart manual contact angle goniometer (model 100). Contact angle measurements were taken using a sessile drop technique, where advancing and receding contact angles were collected by increasing and decreasing the volume of a ∼5 μL drop, respectively. All measurements were taken at room temperature. Data are from at least three measurements on at least nine samples, and the values are reported as the mean ± standard deviation.

Potential-Dependent Contact Angle Goniometry. A standard three-electrode electrochemical cell was built with monolayer-coated gold substrate as the working electrode, an Ag/AgCl wire as a pseudo reference, and a platinum wire as the counter electrode.[7] Contact angles measurements were taken using a Rame-Hart manual contact angle goniometer (model 100), while the potential was applied to the substrate within a ∼5 μL 0.1 M KCl drop (pH adjusted to 11 with KOH). The potential of the gold substrate, relative to the Ag/AgCl wire, was controlled with a Reference 600 potentiostat (Gamry Instruments).

Advancing and receding contact angles were collected by increasing and decreasing the volume of a ∼5 μL drop, respectively. The potential was switched between −0.1 and 0.290 V (reported as negative and positive potential in the text, respectively) with respect to the pseudo Ag/AgCl reference electrode. The elapsed time between potential change and angle measurement was not explicitly measured, but it is estimated to be approximately 20 s. At each potential step, the volume of the drop was increased and then decreased. The applied potential was within the range of stability of studied monolayers on gold.[23,29] The potential of the pseudo reference electrode was measured to be 0.20 ± 0.05 V with respect to a standard Ag/AgCl reference electrode. Data are from at least three measurements on at least six samples, and the values are reported as the mean ± standard deviation.

Micropatterning of Low-Density Monolayers. A SAM of 1,10-decanedithiol was formed on the gold substrate in hexane, as described above. The substrate and mask were separated by 40 μm spacers from one another and the gap in between was filled with an ethanolic solution containing 10-undecynoic acid (50 mM), eosin Y (2.5 mM), and 20 vol % DI water (Figure 2b). The SAM covered surface was

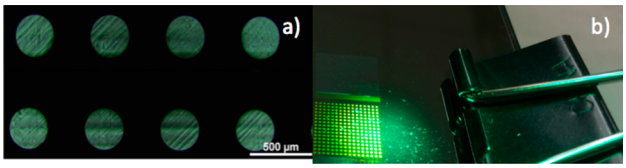

Figure 2. (a) Close-up view of mask used for photopatterning. (b) Irradiation of the monolayer-coated gold substrate through mask with 530 nm light.

then irradiated through a mask (Figure 2a) with 530 nm light with the intensity of 50 mW/cm^2 for 10 min. After disassembly of the mask−substrate system, the substrate was rinsed in a stream of ethanol and then briefly immersed in ethanol for visualization of the pattern. As the gold substrate was removed from the ethanol, the pattern was observed through selective wetting of the patterned regions of the surface.

RESULTS AND DISCUSSION

The overall goal of this work is to demonstrate a simplified, patternable approach to create a stable monolayer with a reduced density of chains at the surface. The photomediated, thiol−yne grafting of an acid-terminated alkyne ligand to a dithiol monolayer is expected to yield a surface with a densely packed base monolayer and an environment-interfacing region of reduced lateral packing density. The overall structure of the undecynoic acid grafted surface was supported by comparing our acid terminated thiol−yne grafting product to control monolayers. A control system with the optimal 2:1 thiol to alkyne grafting was prepared according to solution phase synthesis of a thiol−yne adsorbate (Figure 1b), as previously described.[7] A standard, well-packed decanedithiol SAM was used to relate to the expected structure of the dithiol base layer,

DOI: 10.1021/acs.langmuir.5b00001
Langmuir XXXX, XXX, XXX−XXX

and a well-packed mercaptoundecanoic acid SAM was used to contrast the properties of our acid-terminated, LD-SAM with that of an acid-terminated, well-packed SAM.

Monolayer Interaction with the Environment. Our first objective is to demonstrate a low packing density at the surface for our alkyne grafting approach. We used advancing and receding contact angles of water to investigate the chemical structure of the top several angstroms[30] of the solid-phase product monolayer (Table 1). The advancing contact angle for solid-phase product LD-SAM is 85 ± 2°. The higher advancing contact angle of the solid-phase LD-SAM compared to that of a solution-phase LD-SAM (~65 ± 3°) is consistent with a lower density of carboxylate groups at the surface and a larger contribution from the underlying methylene functionality. To further elucidate the chemical composition at the surface, we calculate the relative contribution of these functionalities with the Cassie equation (eq 2)[6]

Table 1. Advancing and Receding Water Contact Angles (deg) for Monolayers on Gold

monolayer	θ_A	θ_R
11-mercaptoundecanoic acid (MUA)	26 ± 6	12 ± 7
polyethylene[31]	101 ± 3	no data
solution-phase product LD-SAM	65 ± 3	34 ± 4
solid-phase product LD-SAM	85 ± 2	50 ± 2

$$\cos(\theta_{\text{solid-phase LDM}}) = \varphi_{\text{COOH}} \cos(\theta_{\text{COOH}}) + (1 - \varphi_{\text{COOH}}) \cos(\theta_{\text{CH}_2}) \quad (2)$$

where φ_{COOH} denotes the fraction of the surface with carboxyl functionality, $\theta_{\text{solid-phase LDM}}$ is the contact angle of the solid-phase product monolayer, θ_{COOH} is the contact angle of a pure carboxylate surface, and θ_{CH_2} is the contact angle on a polyethylene surface. From eq 2, we estimate that approximately 26 ± 3% of the mixed surface of solid-phase LD-SAM is covered by acid functionalities and the remainder by methylene functionality. This is lower than the theoretical prediction of 2:1 thiol−yne complete grafting, which would yield 50% surface coverage of the carboxylate groups. The low grafting efficiency of the solid-phase approach could be the result of the steric congestion,[11,12] which would limit the accessibility of alkynes to surface bound thiols.

One of the most commonly observed phenomena of low-density monolayers is the potential-dependent change in receding contact angle. Low-density monolayers show reversible macroscopic changes in surface properties because of synergistic molecular reorientations that occur when the substrate is exposed to an external stimulus.[23,32] For a densely packed surface, the structures do not have sufficient space to remodel, and a potential-dependent change in contact angle is not observed.[7] Therefore, a responsive change in the receding contact angle supports a lower density of chains at the surface by demonstrating a capacity for molecular remodeling at the water interface. These changes are more dramatic in the receding contact angle, owing to the strong dependency of the receding angle on the hydrophilic character of the surface. The receding phase boundary is pinned by hydrophilic domains, and the conformation of adsorbates in these regions is altered by the applied potential; the resulting change in hydrophilic character alters the pinning of the receding phase boundary.[33,34]

Advancing and receding contact angles were measured for a low-density monolayer coated gold electrode, in an aqueous solution of 0.1 M KCl (pH 11). Data were taken for five subsequent cycles when the potential to the gold substrate was switched between −0.1 and +0.29 mV with respect to Ag/AgCl (Figure 3). A reversible change in receding contact angle is observed for the solid phase LD-SAM (Figure 3a), while switching is not observed for a well-packed, acid-terminated SAM.[7] The applied potential is in the stability range for alkanethiolate SAMs on gold,[29,35] preventing the reductive desorption of the thiolates from the surface. This is further supported by the reversibility of the measurements, where any desorption would cause irreversible changes in the contact angle. The measured value for the receding contact angle of solid-phase product is 68 ± 1° at an applied potential of +0.29 mV and 55 ± 1° at an applied potential of 0.1 mV. The magnitude of receding contact angle change for solid-phase product (~13°) is comparable to that reported previously for low-density monolayers with 50% chain density of carbonyl groups (~10°).[17,19] Taken together, the traditional and potential-dependent contact angle analysis supports the lower surface density of carboxyl groups in a solid-phase LD-SAM.

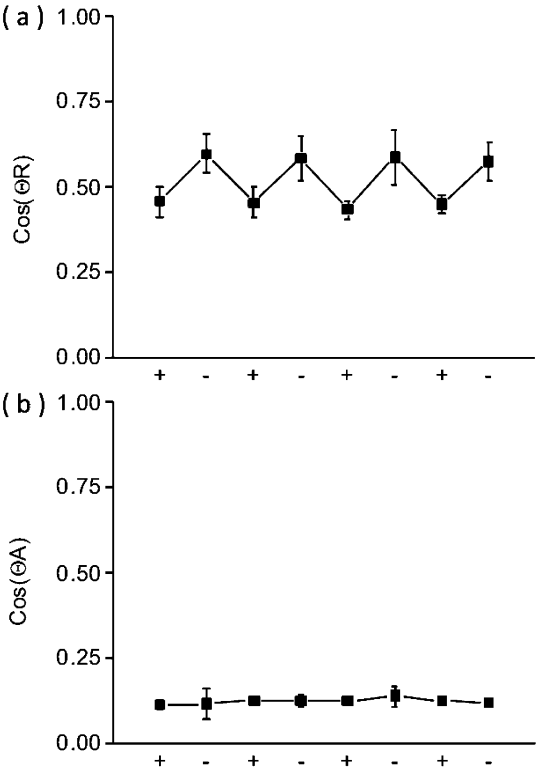

Figure 3. Cosine of (a) receding and (b) advancing contact angles for low-density monolayers prepared by solid-phase thiol−yne grafting. Data were taken while applying either +0.29 or −0.1 mV with respct to Ag/AgCl to a monolayer-coated gold working electrode.

Overall Structure of Solid-Phase LD-SAM. A comparison of the ellipsometric thickness of the solid-phase LD-SAM to that of the control SAMs provides insight into the structure of the solid phase LD-SAM. A standard well-packed 1,10-decanedithiol SAM is 19 Å (Table 2), and this provides a thickness estimate for the lower layer of our solid-phase product LD-SAM. Any additional thickness for the solid-phased LD-SAM is attributed to the grafting of an undecynoic acid

DOI: 10.1021/acs.langmuir.5b00001
Langmuir XXXX, XXX, XXX−XXX

Table 2. Ellipsometric Thickness of Monolayers

monolayer	thickness (Å)
11-mercaptoundecanoic acid (MUA)	16 ± 3
1,10-decanedithiol	19 ± 2
solution-phase product LD-SAM	28 ± 2
solid-phase product LD-SAM	24 ± 1

ligand. If the undecynoic acid layer were densely packed, it would have the approximate thickness of a well-packed 11-mercaptoundecanoic acid SAM (~16 Å). By determining the fractional thickness of the undecynoic acid layer (100% = 16 Å) on top of the 1,10-decanedithiol base layer (19 Å), we estimate a lateral packing density of the undecyoic acid layer to be 31 ± 6% of a densely packed layer. The surface density estimate of the solid-phase LD-SAM is in close agreement with our surface coverage estimate based on surface energy analysis (26 ± 3%).

The low packing density is further supported by grazing angle FTIR analysis. Grazing angle FTIR is a common technique to investigate the chemical composition and aggregate structuring of thin films. Figure 4 shows the

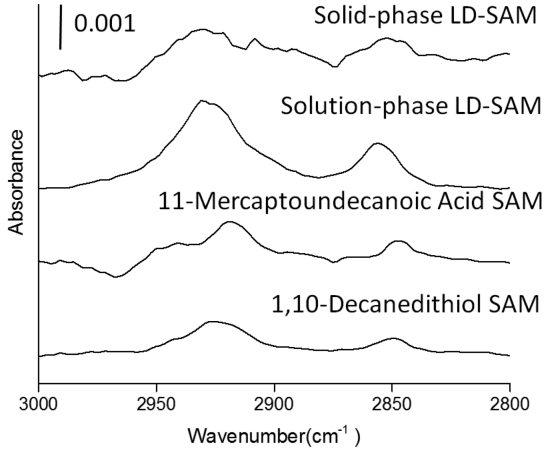

Figure 4. Representative methylene stretching region, $\nu_{as}(CH_2)$ and $\nu_s(CH_2)$, of the FTIR spectra for the solid-phase and solution-phase product low-density monolayer, 11-mercaptoundecanoic acid monolayer, and 1,10-decanedithiol monolayer. The spectra have been offset vertically for clarity.

methylene stretching region of the FTIR spectra for solid-phase product low-density monolayer. The methylene stretching peak positions for solid-phase product LD-SAM (ν_{as} = 2935 cm^{-1} and ν_s = 2856 cm^{-1}) clearly contrast with that of a well-packed 11-mercaptoundecanoic acid SAM, where the peaks associated with asymmetric and symmetric stretching have shifted toward higher wavenumbers from what is seen for well-packed SAM (2918 and 2849 cm^{-1}, respectively).[36] The shift toward higher wavenumber in the methylene region is commonly interpreted as a decrease in overall crystallinity for the methylene regions of monolayer, supporting a more disordered overall methylene region for the solid-phase product monolayer when compared to a traditional SAM. This trend is consistent with other studies of altered monolayer packing.[18,19,36] The asymmetric and symmetric methylene stretching peaks for solid-phase product are even more disordered (higher wavenumber) than the solution-phase thiol−yne surfaces (2928 and 2853 cm^{-1}, respectively). The lower overall crystallinity of solid-phase product monolayer when compared to the optimal structure of the solution-phase LD-SAM is consistent with both a lower chain density and a potential disruption of the methylene packing in the dithiol base layer.

To further evaluate the potential disruption of the dithiol base layer, we studied the electrochemical barrier properties of the coating. Based on the fits of impedance spectra by the Randles model (Figure S1 of the Supporting Information), estimates of the monolayer's resistance and capacitance were determined and are compiled in Table 3 and Figure 5. Nyquist

Table 3. Values for Monolayer Resistance and Capacitance

monolayer	log(R_f) (Ω cm^2)	C_f (μF/cm^2)
11-mercaptoundecanoic acid (MUA)	4.9 ± 0.3	2.8 ± 0.4
1,10-decanedithiol	4.8 ± 0.6	2.7 ± 0.3
solution-phase product	5.3 ± 0.3	1.5 ± 0.2
solid-phase product	4.1 ± 0.5	4.1 ± 1.1

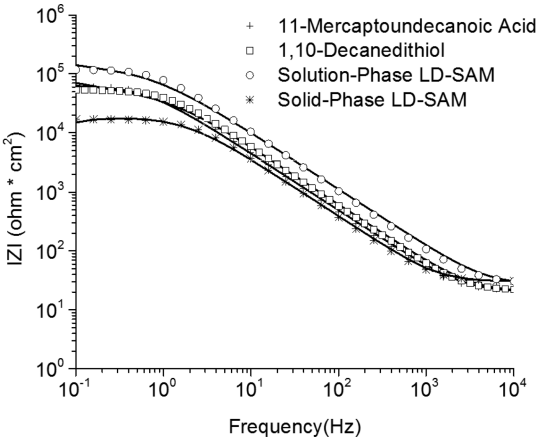

Figure 5. Electrochemical impedance spectra obtained in an aqueous solution of 1 mM $K_3[Fe(CN)_6]$, 1 mM $K_4[Fe(CN)_6]$, and 0.1 M Na_2SO_4 for monolayers prepared on gold. Experimental results are shown as symbols, where lines are fits of circuit models to the data.

plots are provided as Figure S2 of the Supporting Information. The majority of the resistance to charge transfer across a thiol−yne LD-SAM monolayer is afforded by the lower-phase well-packed structure, as the upper phase has a loose, poorly organized structure. If the structuring of the dithiol base layer is undisturbed by the solid-phase grafting of undecynoic acid, we would expect that the product LD-SAM will have a comparable resistance to ion transport as traditional well-packed monolayer of 1,10-decanedithiol.[7] A densely packed base layer is clearly observed in the solution-phase thiol−yne SAM, where the solution-phase product LD-SAM (~$10^{5.3}$ Ω cm^2) is comparable to that of a 1,10-decanedithiol SAM (~$10^{4.8}$ Ω cm^2). This is contrasted with the measured film resistance for solid-phase product LD-SAM (~$10^{4.1}$ Ω cm^2), where the lower film resistance for solid-phase product LD-SAM (p-value <10^{-11}) indicates the presence of gaps between alkanethiolate chains at the gold interface.

Film capacitance also provides an insight into the structuring of these monolayer systems. In most monolayer systems, the film capacitance is roughly proportional to the inverse of film thickness. Therefore, as the monolayer gets thicker, it is expected that capacitance gets smaller. For the proposed structure, the solid-phase LD-SAM is expected to have a higher thickness than the control well-packed MUA or decanedithiol monolayers. Instead, the capacitance for solid-phase product

DOI: 10.1021/acs.langmuir.5b00001
Langmuir XXXX, XXX, XXX−XXX

Table 4. Reductive Desorption Analysis of Surface Chain Density and Stability

monolayer	$Q_{Au\text{-}SR}$ (μC/cm^2)	density of chains at Au (nm^2/molecule)	peak positions (V vs Ag/AgCl)
11-mercaptoundecanoic acid (MUA)	92.1 ± 7.4	0.18 ± 0.01	−0.86 ± 0.06
solution-phase product	86.8 ± 6.0	0.19 ± 0.01	−1.01 ± 0.02
solid-phase product	88.4 ± 7.3	0.18 ± 0.02	−0.96 ± 0.01

LD-SAM (~4.10 μF) is higher than that of MUA (~2.75 μF) and 1,10-decanedithiol (~2.66 μF). This unexpectedly high interfacial capacitance is supportive of defects in the coating, potentially attributed to the partial desorption of alkanethiolates from gold surface.

Both FTIR and electrochemical impedance analysis are consistent with a disruption of the dithiol base layer of the solid phase LD-SAM. Any disruption to the base layer would require a lower density of thiol−gold bonds at the gold surface to allow space for noncrystalline chain conformations. Alkanethiolates desorb from gold substrate through one-electron reduction process in alkaline solution.[37,38] To further investigate the base structure of the solid-phase product LD-SAM at gold, the density of alkanethiolate chains at surface was determined from the total electrical charge required for desorption of monolayer from the gold.[37,39] The chain density at the gold interface is expected to be consistent with that of a well-packed monolayer with analogous base structure. Using a potentiostat, the potential of a monolayer-coated gold working electrode was swept from 0.345 to −1.545 V vs Ag/AgCl in 0.5 M KOH electrolyte at 100 mV/s. The surface coverages of the studied monolayers are summarized in Table 4.

The mean surface chain density for the solid phase LD-SAM is equivalent to that of either a solution-phase LD-SAM or a well-packed MUA due to similar base structure. Critically, the standard deviation of the measurement accounts for 11% of the mean chain density, and this measurement is insensitive to a small proportion of dithiol adsorbates which may have desorbed from the gold substrate. Given the lower electrochemical resistance for ion-transport as shown with EIS, it is likely that there is some loss of structuring in the dithiol layer in the solid phase LD-SAM, but the magnitude of this loss is below the limit of detection by reductive desorption in these systems.

The cyclic voltammograms of solid-phase LD-SAMs and MUA monolayers exhibit a broad peak at −1.1 V (Figure 6). These peaks are observed in other reports of the reductive desorption of thiolates from annealed gold substrates.[40−42] The more negative desorption peak on the voltammograms is attributed to the field-induced rearrangements of surface domains within the electrical double layer.[40] On the basis of these prior studies, we interpret the less negative peak as resulting from the cleavage of the gold−sulfur bond. This interpretation is further supported by both the expected position of the MUA desorption and the sharpness of the desorption peak,[19] while the more negative peak is likely due to the previously reported, field-induced rearrangement of adlayer domains.[40]

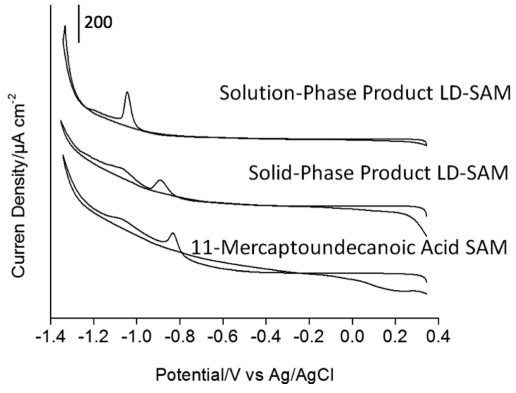

Figure 6. Cyclic voltammograms obtained for studied monolayers in 0.5 M KOH as potential was swept at scan rate of 0.1 V s^{-1} from 0.345 to −1.545 V vs Ag/AgCl reference electrode. Spectra are offset vertically for clarity.

Stability of Solid-Phase LD-SAM. Long-term electrochemical stability is essential to many applications of low-density monolayers, and the process of preparing LD-SAMs with long stability over time is challenging. It has been shown by Lahann and co-workers[23] that acid-terminated LD-SAMs prepared through a cleavage-base technique have a significant decrease in alkyl chain fluidity over the course of 4 weeks storage because of increased ordering of alkyl chains on the surface.[18] Additionally, the acid-terminated LD-SAMs prepared by noncovalent interactions of ion pairs in solution (Figure 1c)[17] were less electrochemically stable than their well-packed mercaptohexadecanoic acid counterparts, which is caused by weak intermolecular interactions of the LD-SAMs.[19]

In a reductive desorption analysis of the electrochemical stability of monolayers, the cathodic peak is observed at −0.96 V for solid-phase product LD-SAM. This postion is more negative than the potential observed for the well-packed MUA monolayer (−0.86 V, Table 4 and Figure 6). The increase in required potential to desorb the molecules is commonly interpreted as an increase in overall stability of monolayer.[19,32,43,44] EIS supports a disrupted base dithiol layer in the solid-phase LD-SAM (Table 3), which should result in a lowering of the electrochemical stability of the solid-phase LD-SAM. Since the electrochemical stability of this coating is greater than that of a defect-free conventional monolayer, there must be an additional stabilizing contribution to the film structure to overcome the poorly ordered base layer. These observations strongly support the structure of this coating contains doubly bound adsorbates similar to that of the idealized control (solution phase LD-SAM).

We also contrasted the reductive desorption data for solid-phase product LD-SAM to that of solution-phase product LD-SAM (Table 4 and Figure 6). The position of the solution-phase LD-SAM reduction peak was more negative than the solid-phase LD-SAM. This lower stability of solid-phase LD-SAMs further supports the likely partial desorption of thiolates from the gold substrate. As described in our previous work,[7] the two thiol−gold linkage per adsorbate resulted in ~50% surface coverage of carbonyl groups for solution-phase product LD-SAM and had a major effect on enhancing the stability of product monolayer. As the solid-phase product LD-SAM only achieves ~30% surface coverage, the number of doubly bound adsorbates is lower, and the potential to cleave the monolayer from gold surface is less negative.

DOI: 10.1021/acs.langmuir.5b00001
Langmuir XXXX, XXX, XXX−XXX

Surface Photopatterning via Thiol−Yne Click Reaction. Patterned, densely packed SAMs have sophisticated microscale features which provide well-characterized supports for physicochemical and biochemical processes.[45] Thiol−yne grafting provides a general, patternable method to prepare low-density monolayers with diverse terminal chemical functionalities and exceptional stability. Using light-initiated thiol−yne grafting reaction, we introduce patterned features into dithiol monolayer-coated gold substrates. These structures are expected to be as stable as seen in the large surface area materials studied by reductive desorption, while presenting a low packing density described by complementary surface energy, ellipsometry, and FTIR analyses.

Here, we graft undecynoic acid terminal groups to only the regions irradiated with collimated 530 nm light. The chrome-coated quartz photomask used here consists of a square grid of 200 μm circular openings (Figure 7a). After grafting, the surface was rinsed in a stream of ethanol and then briefly dipped in ethanol. Upon exiting the ethanol, the ethanol selectively wetted the carboxyl functionalized domains owing to the contrast in surface energy with the unirradiated, thiol-terminated regions (Figure 7b).

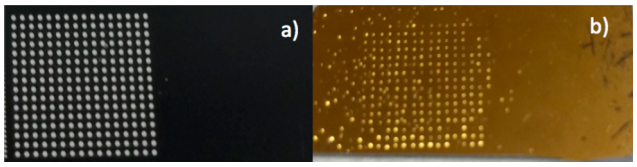

Figure 7. Photopatterning of thiol−yne grafting reaction for micropatterning of a stable, low-density monolayer on gold. (a) Mask used for photoirradiation. (b) Site-selective formation of ethanol droplets obtained by dipping the patterned surfaces in ethanol.

CONCLUSIONS

Highly stable, low-density self-assembled monolayers on gold were prepared through thiol−yne click chemistry between alkyne ligands and thiol-terminated organic monolayers. The product monolayer has a two-layer structure with a highly crystalline phase adjacent to gold substrate similar to a well-packed SAM. The product LD-SAMs were compared to that of an acid-terminated well-packed monolayer and LD-SAMs prepared through a previously reported solution-phase approach. Analysis of surface energy, ellipsometry, FTIR, and EIS support our claimed structure for the resulting monolayer and suggest a partial desorption of thiolates from the thiol-terminated monolayer head phase. The reductive desorption data show that the solid-phase product LD-SAMs are more electrochemically stable than well-packed MUA SAMs, while they are less stable than LD-SAMs prepared by the solution-phase approach. Both solution-phase and solid-phase LD-SAM approaches result in LD-SAMs with high stability when compared to a well-packed SAM. This approach is expected to be compatible with varied tail group functionalities. While the solution-phase approach results in more electrochemically stable LD-SAMs, with higher surface coverage of desired chemical functionalities, it requires the chemical synthesis of adsorbates and is more experimentally challenging. The solid-phase approach allows for faster and simpler preparation of LD-SAMs, but with less precision in surface coverage and distribution of chemical functionalities. Finally, it is simple to photopattern the grafting of acid terminated alkynes to a 1,10-decanedithiol-covered gold substrate using this general solid phase approach.

ASSOCIATED CONTENT

Supporting Information

Details of the Randles circuit model employed to fit the EIS data along with the parameters and equations used for fits; Nyquist plots of prepared LD-SAMs, 1,10-decanedithiol SAM, and 11-mercaptoundecanoic acid SAM. This material is available free of charge via the Internet at http://pubs.acs.org.

AUTHOR INFORMATION

Corresponding Author

*E-mail: brad.berron@uky.edu (B.J.B.).

Notes

The authors declare no competing financial interest.

ACKNOWLEDGMENTS

Acknowledgment is made to the Donors of the American Chemical Society Petroleum Research Fund (52743-DNI5) for partial support of this research. The authors also acknowledge UK Center for Nanoscale Science and Engineering for use of a sputtering machine and a spectroscopic ellipsometer.

ABBREVIATIONS

SAM, self-assembled monolayer; LD-SAM, low-density self-assembled monolayer; MUA, mercaptoundecanoic acid; FTIR, Fourier transform infrared spectroscopy; EIS, electrochemical impedance spectroscopy.

REFERENCES

(1) Prashar, D. Self assembled monolayers-A review. *Int. J. ChemTech Res.* **2012**, *4* (1), 258−265.

(2) Porter, M. D.; Bright, T. B.; Allara, D. L.; Chidsey, C. E. D. Spontaneously organized molecular assemblies. 4. Structural characterization of normal-alkyl thiol monolayers on gold by optical ellipsometry, infrared-spectroscopy, and electrochemistry. *J. Am. Chem. Soc.* **1987**, *109* (12), 3559−3568.

(3) Laibinis, P. E.; Whitesides, G. M.; Allara, D. L.; Tao, Y. T.; Parikh, A. N.; Nuzzo, R. G. Comparison of the structures and wetting properties of self-assembled monolayers of normal-alkanethiols on the coinage metal-surfaces, Cu, Ag, Au. *J. Am. Chem. Soc.* **1991**, *113* (19), 7152−7167.

(4) Schlenoff, J. B.; Li, M.; Ly, H. Stability and self-exchange in alkanethiol monolayers. *J. Am. Chem. Soc.* **1995**, *117*, 12528−12536.

(5) Love, C. J.; Estroff, L. A.; Kriebel, J. K.; Nuzzo, R. G.; Whitesides, G. M. Self-assembled monolayers of thiolates on metals as a form of nanotechnology. *Chem. Rev.* **2005**, *105* (4), 1103−1170.

(6) Laibinis, P. E.; Palmer, B. J.; Lee, S.-W.; Jennings, G. K. The synthesis of organothiols and their assembly into monolayers on gold. *Thin Films* **1998**, *24*, 2−43.

(7) Stevens, C. A.; Safazadeh, L.; Berron, B. J. Thiol-yne adsorbates for stable, low-density, self-assembled monolayers on gold. *Langmuir* **2014**, *30* (8), 1949−1956.

(8) Folkers, J. P.; Laibinis, P. E.; Whitesides, G. M. Self-assembled monolayers of alkanethiols on gold: comparisons of monolayers containing mixtures of short- and long-chain constituents with methyl and hydroxymethyl terminal groups. *Langmuir* **1992**, *8*, 1330−1341.

(9) Bain, C. D.; Whitesides, G. M. Formation of monolayers by the coadsorption of thiols on gold - Variation in the length of the alkyl chain. *J. Am. Chem. Soc.* **1989**, *111* (18), 7164−7175.

(10) Laibinis, P. E.; Whitesides, G. M. Omega-terminated alkanethiolate monolayers on surfaces of copper, silver, and gold have similar wettabilities. *J. Am. Chem. Soc.* **1992**, *114* (6), 1990−1995.

DOI: 10.1021/acs.langmuir.5b00001
Langmuir XXXX, XXX, XXX−XXX

(11) Sullivan, T. P.; Huck, W. T. S. Reactions on monolayers: Organic synthesis in two dimensions. *Eur. J. Org. Chem.* **2003**, *2003* (1), 17−29.
(12) Alexander, M. R.; Wright, P. V.; Ratner, B. D. Trifluoroethanol derivatization of carboxylic acid-containing polymers for quantitative XPS analysis. *Surf. Interface Anal.* **1996**, *24* (3), 217−220.
(13) Choi, E. J.; Foster, M. D. The role of specific binding in human serum albumin adsorption to self-assembled monolayers. *Langmuir* **2002**, *18*, 557−561.
(14) Garg, N.; Lee, T. R. Self-assembled monolayers based on chelating aromatic dithiols on gold. *Langmuir* **1998**, *14* (14), 3815−3819.
(15) Park, J. S.; Smith, A. C.; Lee, T. R. Loosely packed self-assembled monolayers on gold generated from 2-alkyl-2-methylpropane-1,3-dithiols. *Langmuir* **2004**, *20* (14), 5829−5836.
(16) Park, J. S.; Vo, A. N.; Barriet, D.; Shon, Y. S.; Lee, T. R. Systematic control of the packing density of self-assembled monolayers using bidentate and tridentate chelating alkanethiols. *Langmuir* **2005**, *21* (7), 2902−2911.
(17) Olivier, G. K.; Shin, D.; Gilbert, J. B.; Monzon, L. M.; Frechette, J. Supramolecular ion-pair interactions to control monolayer assembly. *Langmuir* **2009**, *25* (4), 2159−2165.
(18) Peng, D.; Lahann, J. Chemical, electrochemical, and structural stability of low-density self-assembled monolayers. *Langmuir* **2007**, *23* (20), 10184−10189.
(19) Luo, M.; Frechette, J. Electrochemical stability of low-density carboxylic acid terminated monolayers. *J. Phys. Chem. C* **2010**, *114* (47), 20167−20172.
(20) Lowe, A. B. Thiol-yne 'click'/coupling chemistry and recent applications in polymer and materials synthesis and modification. *Polymer* **2014**, *55*, 5517−5549.
(21) Lowe, A. B.; Hoyle, C. E.; Bowman, C. N. Thiol-yne click chemistry: A powerful and versatile methodology for materials synthesis. *J. Mater. Chem.* **2010**, *20*, 4745−4750.
(22) Hoogenboom, R. Thiol-yne chemistry: a powerful tool for creating highly functional materials. *Angew. Chem., Int. Ed.* **2010**, *49* (20), 3415−3417.
(23) Lahann, J.; Mitragotri, S.; Tran, T.-N.; Kaido, H.; Sundaram, J.; Choi, I.; Hoffer, S.; Somorjai, G.; Langer, R. A reversibly switching surface. *Science* **2003**, *299* (5605), 371−374.
(24) Shon, Y. S.; Lee, T. R. Desorption and exchange of self-assembled monolayers (SAMs) on gold generated from chelating alkanedithiols. *J. Phys. Chem. B* **2000**, *104* (34), 8192−8200.
(25) Merrifield, R. B. Solid phase peptide synthesis. I. The synthesis of a tetrapeptide. *J. Am. Chem. Soc.* **1963**, *85* (14), 2149−2154.
(26) Cokbaglan, L.; Arsu, N.; Yagci, Y.; Jockusch, S.; Turro, N. J. 2-Mercaptothioxanthone as a novel photoinitiator for free radical polymerization. *Macromolecules* **2003**, *36* (8), 2649−2653.
(27) Temel, G.; Karaca, N.; Arsu, N. Synthesis of main chain polymeric benzophenone photoinitiator via thiol-ene click chemistry and Its use in free radical polymerization. *J. Polym. Sci., Part A: Polym. Chem.* **2010**, *48* (23), 5306−5312.
(28) Karasu, F.; Arsu, N.; Jockusch, S.; Turro, N. J. Mechanistic studies of photoinitiated free radical polymerization using a bifunctional thioxanthone acetic acid derivative as photoinitiator. *Macromolecules* **2009**, *42* (19), 7318−7323.
(29) Russell Everett, W.; Fritsch-Faules, I. Factors that influence the stability of self-assembled organothiols on gold under electrochemical conditions. *Anal. Chim. Acta* **1995**, *307* (2), 253−268.
(30) Cooper, S. L.; Bamford, C. H.; Tsurata, T. Polymer biomaterials in solution, as interfaces and as solids. *J. Biomed. Mater. Res.* **1996**, *30* (2), 171.
(31) Xiaoying, L.; Changchun, Z.; Yanchun, H. Low-density polyethylene superhydrophobic surface by control of its crystallization behavior. *Macromol. Rapid Commun.* **2004**, *25* (18), 1606−1610.
(32) Luo, M.; Amegashie, A.; Chua, A.; Olivier, G. K; Frechette, J. Role of solution and surface coverage on voltage-induced response of low-density self-assembled monolayers. *J. Phys. Chem. C* **2012**, *116* (26), 13964−13971.
(33) Drelich, J.; Miller, J. D.; Good, R. J. The effect of drop (bubble) size on advancing and receding contact angles for heterogeneous and rough solid surfaces as observed with sessile-drop and captive-bubble techniques. *J. Colloid Interface Sci.* **1996**, *179* (1), 37−50.
(34) Drelich, J.; Wilbur, J. L.; Miller, J. D.; Whitesides, G. M. Contact angles for liquid drops at a model heterogeneous surface consisting of alternating and parallel hydrophobic/hydrophilic strips. *Langmuir* **1996**, *12* (7), 1913−1922.
(35) Finklea, H. O.; Avery, S.; Lynch, M.; Furtsch, T. Blocking oriented monolayers of alkyl mercaptans on gold electrodes. *Langmuir* **1987**, *3* (3), 409−413.
(36) Berron, B.; Jennings, G. Loosely packed hydroxyl-terminated SAMs on gold. *Langmuir* **2006**, *22* (17), 7235−7240.
(37) Sumi, T.; Wano, H.; Uosaki, K. Electrochemical oxidative adsorption and reductive desorption of a self-assembled monolayer of decanethiol on the Au (111) surface in KOH + ethanol solution. *J. Electroanal. Chem.* **2003**, *550*, 321−325.
(38) Widrig, C. A.; Chung, C.; Porter, M. D. The electrochemical desorption of n-alkanethiol monolayers from polycrystalline Au and Ag electrodes. *J. Electroanal. Chem.* **1991**, *310* (1), 335−359.
(39) Sumi, T.; Uosaki, K. Electrochemical oxidative formation and reductive desorption of a self-assembled monolayer of decanethiol on a Au(111) surface in KOH ethanol solution. *J. Phys. Chem. B* **2004**, *108* (20), 6422−6428.
(40) Yang, W.; Gooding, J. J.; Hibbert, D. B. Characterisation of gold electrodes modified with self-assembled monolayers of L-cysteine for the adsorptive stripping analysis of copper. *J. Electroanal. Chem.* **2001**, *516* (1-2), 10−16.
(41) Tudos, A. J.; Johnson, D. C. Dissolution of gold electrodes in alkaline media containing cysteine. *Anal. Chem.* **1995**, *67* (3), 557−560.
(42) Yang, D. F.; Wilde, C. P.; Morin, M. Studies of the electrochemical removal and efficient re-formation of a monolayer of hexadecanethiol self-assembled at an Au(111) single crystal in aqueous solutions. *Langmuir* **1997**, *13* (2), 243−249.
(43) Yang, D. F.; Wilde, C. P.; Morin, M. Electrochemical desorption and adsorption of nonyl mercaptan at gold single crystal electrode surfaces. *Langmuir* **1996**, *12* (26), 6570−6577.
(44) Pesika, N. S.; Stebe, K. J.; Searson, P. C. Kinetics of desorption of alkanethiolates on gold. *Langmuir* **2006**, *22* (8), 3474−3476.
(45) Smith, R. K.; Lewis, P. A.; Weiss, P. S. Patterning self-assembled monolayers. *Prog. Surf. Sci.* **2004**, *75* (1), 1−68.

DOI: 10.1021/acs.langmuir.5b00001
Langmuir XXXX, XXX, XXX−XXX